Micro and Nano Systems Letters

LETTER

CrossMark

Photolithography of SU-8 microtowers for a 100-turn, 3-D toroidal microinductor

Jungkwun J. K. Kim[*], Hassan Al Thuwaini and Mohammad Almuslem

Abstract

We present a photolithography scheme for ultra-tall, high-aspect-ratio microstructures. While increased height of microstructures can expand the design capability of various microdevices, it has been challenging to achieve the ultra-tall microstructure, 1 mm or higher, using a well-known negative photoresist, SU-8. One of the reasons is the high absorption rate of 365-nm ultra-violet light during the exposure process, although it used to be recommended for the SU-8 process. We report on optical characteristics of microlithography, in particular the 365- and 405-nm wavelengths, and present the lithography method for ultra-tall micropillars with a height of 1 mm or higher, called microtowers. While the 365-nm wavelength is experimentally validated with its high attenuation inside the SU-8, higher transparency of the 405-nm wavelength with a thicker SU-8 is reported to be suitable for ultra-tall micropillar structures. Assuming exposure time causes the color change of the SU-8, transparency of the SU-8 as a function of exposure time is measured with a thick SU-8. SU-8 microtowers with various heights are reported, including an array of 2000-µm-tall microtowers and a state-of-the-art 7000-µm microtower. To demonstrate usefulness of the proposed fabrication method, an array of 1000-µm-tall microtowers are successfully fabricated to form a 100-turn, 3-D toroid inductor. The fabricated inductor shows average inductance of 950 nH in the frequency range of 0.1 to 10 MHz, a low-frequency resistance of 5.4 Ω at 0.1 MHz, and a quality factor of 22 at 60 MHz.

Keywords: Microtower, 3-D toroid inductor, High-aspect ratio, SU-8

Introduction

An epoxy-based negative photoresist, SU-8, has become widespread in microelectronics, and bio, optics, and radio-frequency (RF) research [1–6]. Relatively easy to use, SU-8 is chemically stable and well-known for its mechanical characteristics [7]. Moreover, high-aspect-ratio structures in the hundredths micron scale have demonstrated how various microdevices keep the overall dimension of the microdevices small by effectively utilizing conventionally unused space. For example, an SU-8, pillar-framed metalized monopole antenna holds a small footprint area compared to a conventional 2-D printed design on a circuit board [8, 9]; while the expanded height of the antenna allows for more extensive frequency selection. We used an array of SU-8 pillars for micromachined 3-D toroid inductors [10–13]. For these microinductors,

we used 600- to 1000-µm support materials, including an SU-8 pillar array. However, performance of the antenna or the inductor could be expanded with a taller height and higher-aspect ratio of the SU-8 structures.

Two significant challenges arise when fabricating a 1-mm or taller microstructure. The first is optical transparency with 365-nm UV light. Shorter wavelengths attenuate faster in general, and the 365-nm UV light is mostly absorbed in a few hundredths of micron depth in the SU-8 as depicted in Fig. 1. It is advantageous to have this few hundredths micron thickness of SU-8 because most of 365-nm energy can quickly crosslink. However, it may not be suitable for the millimeter-scale SU-8 process.

Another challenge is diffraction, as the tall SU-8 structure typically requires high energy and thereby a long exposure time. Since most lithography systems emit polychromic light with peaks of 365 nm, 405 nm, and 436 nm, diffraction from different wavelengths with a long exposure may cause a crosslinking of SU-8,

*Correspondence: jkkim1324@ksu.edu
Department of Electrical and Computer Engineering, Kansas State University, Manhattan, USA

Kim *et al. Micro and Nano Syst Lett* (2018) 6:14

Page 2 of 9
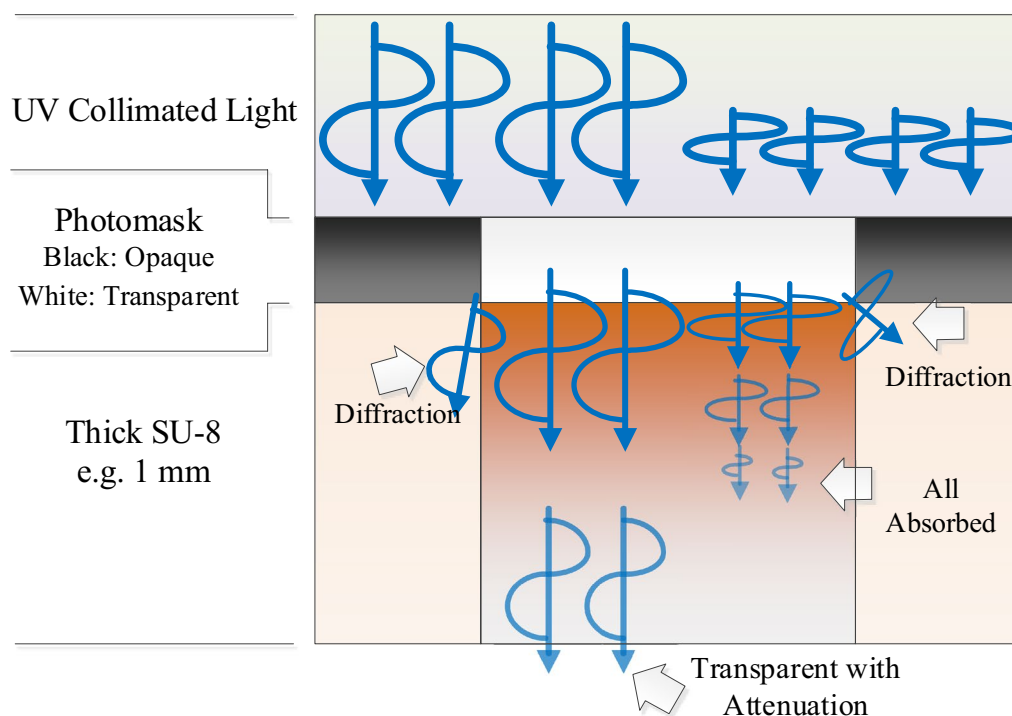
Fig. 1 Description of a short- and long-wavelength UV light propagation during the backside UV exposure for SU-8 pillar fabrication

producing an unwanted sidewall profile as described in Fig. 1. An SU-8 array with 2-mm height was fabricated using typical lithography as shown in Fig. 2. Approximately 20 J of UV energy (OAI, LS-30) was applied using the backside exposure scheme [14–16] with a 100-μ-hole photomask for the exposure. The fabrication result showed the bottom of the pillar had become much larger at nearly 480 μm, compared to the original photomask size of 100 μm. This was presumably caused by the massive energy absorption with multiple wavelengthes at the bottom as short wavelength diffractions were added [17]. Also, the curved sidewall of the pillar was formed.

In this paper, a fabrication method of microtower structures is presented using the mercury-vapor lamp, UV lithography system. To selectively choose the UV wavelength, an acrylic plate was adopted as an optical filter, which passed the UV wavelength of approximately 380 nm or longer [17, 18]. The attenuation of 405-nm UV light as a function of SU-8 thickness was explored. Also, the transparency variation of the 405-nm UV light as a function of exposure time was reported. Microtower arrays, with multiple heights from 1000 to 7000 μm, were fabricated with 405-nm exposure and compared to similar microtower structures with broadband UV exposure. We also demonstrated inclined 3-D microstructures using multidirectional UV lithography [19, 20]. The 3-D

toroidal microinductors utilized the microtower structures at vertical winding as demonstrated. An array of 1000-μm-tall, SU-8 microtowers was implemented for a 100-turn, 3-D microinductor. The fabricated inductor was electrically characterized resulting in an average inductance of 950 nH in the frequency range of 0.1 to 10 MHz.

Optical characteristics of UV lithography

The mercury-vapor lamp in a UV lithography system typically emits a broad spectrum of UV light with three different wavelength peaks including i-, h-, and g-lines (365 nm, 405 nm, and 436 nm, respectively). While the multipeaks of UV lights in the lithography system satisfy various photoresist processes, they often interfere with and result in an unwanted photoresist profile, in particular with thick photoresist fabrication. Figure 2 demonstrates a 2-mm-thick, SU-8 film which was exposed to a UV lithography system (OAI-LS30). Note that SU-8 2025 (MicroChem, Inc.) was used in this experiment. The photomask also served as a substrate for backside exposure. The bottom of the fabricated pillars formed to around 400 μm, which had become nearly four times larger than that of the original 100-μm hole photo pattern. As the short wavelengths, near 365 nm, are quickly absorbed in the SU-8 film, the i-line and shorter wavelengths,

Kim *et al. Micro and Nano Syst Lett*   (2018) 6:14

Page 3 of 9
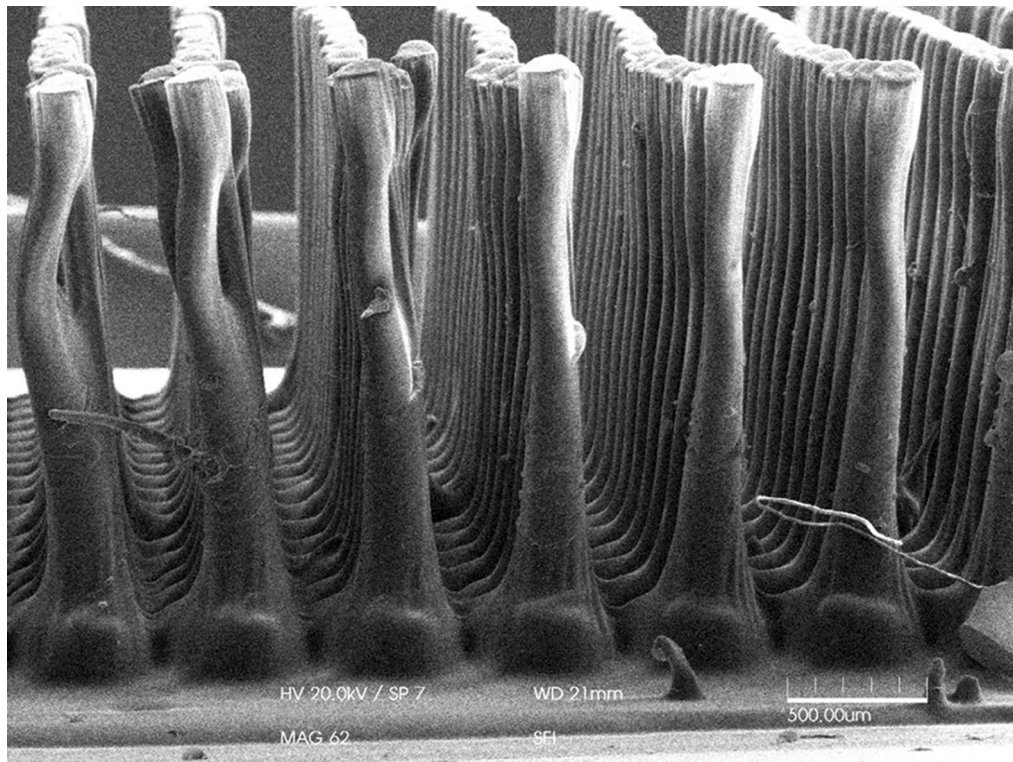
Fig. 2 Conventional lithography for 2000-µm-tall microtowers, resulting in an enlarged bottom and wavy sidewall
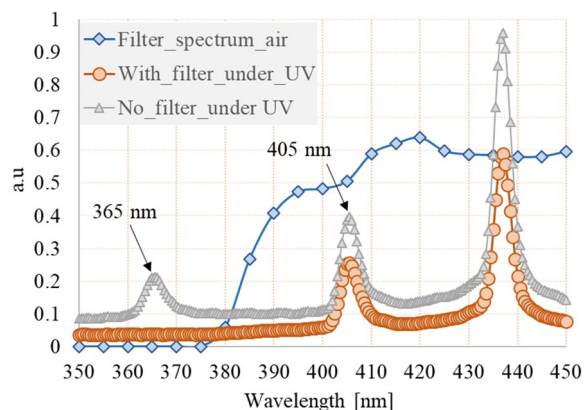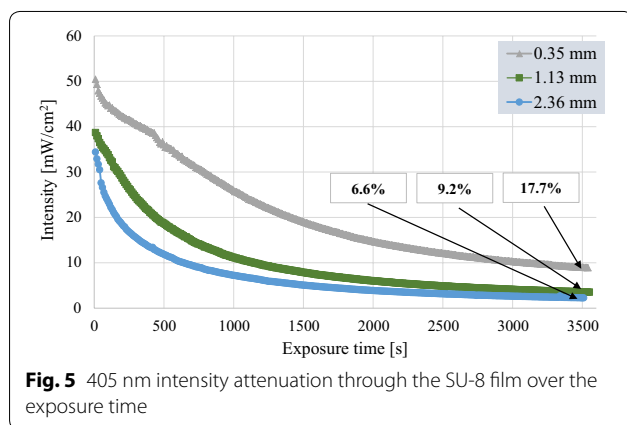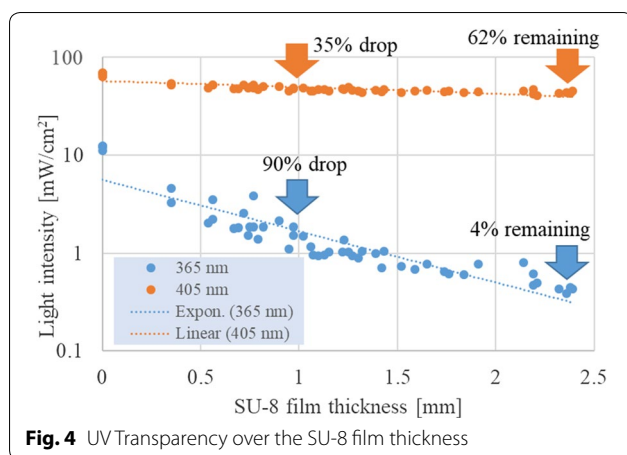

Fig. 3 UV wavelength spectrum measured under a standard UV exposure system: without filter (triangle), with filter (circle), and a spectrum measurement of the filter using a spectrum analyzer (diamond)

including diffracted energy, cause the larger geometry of the pillar structure. To cut off the i-line and shorter wavelengths to form a straight sidewall of the microstructures, a piece of an acrylic plate was adopted as an optical filter [17] and characterized the wavelength filtration as shown in Fig. 3. The transparency of the optical filter (a clear-cast acrylic sheet, McMaster-Carr) was measured in the wavelength range of 340 nm to 450 nm, using a spectrophotometer (Huanghua Faithful Instrument Co. Ltd). The filter showed a transparency of 50% or higher in the wavelength region of 395 nm to 450 nm, and it mostly cut off the wavelength under 375 nm. A spectrum of the UV wavelength in the lithography system (OAI, LS-30) was then measured. The i-, h-, and g-line peaks were shown as expected and as plotted in the triangle dots (gray). The optical filter was inserted under the UV light source and the spectrum was measured, resulting in clearly filtering out the i-line as shown in the red circle plot. As the g-line was considered as visible blue light, the SU-8 process with the introduced filter utilized the narrow band of UV at the 405-nm peak.

Light-intensity attenuation through different SU-8 film thicknesses was also measured in the wavelength selection of i- and h-lines, using an intensity meter (G&R Labs, Model 202) as shown in Fig. 4. Multiple SU-8 samples with different thicknesses ranging from 300 µm to 2.3 mm were tested. Intensity of the i-line through the SU-8 film was mostly attenuated near a 1-mm thickness while the intensity of the h-line was still observed as around 65% of the original intensity. Note that a standard soda-lime glass (Telic Inc., 0.04" thick) was used as

Kim *et al. Micro and Nano Syst Lett*   (2018) 6:14

Page 4 of 9

Fig. 4 UV Transparency over the SU-8 film thickness

Fig. 5 405 nm intensity attenuation through the SU-8 film over the exposure time

a substrate for the SU-8 film, and the intensity attenuation of the glass was compensated by measuring the light intensity without SU-8 film. Approximately 62% of the h-line intensity was shown to have a 2.3-mm-thick SU-8 film while only 4% of the i-line was observed. The experiment results indicated the h-line is suitable for the thick photoresist process.

The transparency variation of the SU-8 film during the UV exposure process was also observed. In the SU-8, the photoacid is produced during the UV exposure process upon the absorption of light. The photoacid as a catalyst causes the crosslinking when the SU-8 film is heated above its glass transition temperature ($T_g = 55°$). This crosslinking of thin negative photoresist usually occurs during the post-exposure bake process. However, long UV exposure time of the thick SU-8 photoresist also causes a partial crosslinking of SU-8 during the UV exposure due to heat accumulation. Figure 5 shows the light-intensity degradation as a function of UV exposure time. SU-8 samples with film thicknesses of 0.35 mm, 1.13 mm, and 2.36 mm were prepared. Each sample was

exposed under the mercury-vapor lamp (OAI, LS-30) for around 3600 s and had its h-line intensity variation measured. The intensity of the 0.35 mm was observed around 9 mW/cm^2 after 3600 s of exposure, which is still a reasonable intensity to activate the crosslinkers. The samples of 1.13 mm and 2.36 mm indicated the h-line intensity around 5 mW/cm^2 after 2400 s and 1500 s of exposure, respectively.

Fabrication process

The fabrication process of the 2-mm-tall SU-8 structures has been described as follows. A backside UV exposure scheme was adopted in this fabrication [10]. A soda lime glass with chromium photomask patterns was prepared as a substrate as well as a photomask. The photomask design included 30-μm-hole-array patterns. An SU-8 2025 was weighed and poured onto the substrate to project the desired SU-8 thickness. Before the SU-8 pouring, a 3-D printed bracket was placed on the edge of the substrate to prevent the photoresist from overflowing. Typically, less than a 2-mm-thick SU-8 process does not require the overflowing protection bracket. Also, an SU-8 dry films can reduce the softbake process as long as the film thickness is suitable for the purpose of the SU-8 process. A softbake was conducted at 95 °C for 15 h. After gently cooling down to room temperature, the sample was flipped and exposed to UV light. During the exposure, a 6.25-mm-thick acrylic filter (Clear Cast Acrylic Sheet, McMaster-Carr) was placed on top of the sample serving as an optical filter. An approximate exposure energy of 290 J/cm^2 was provided to fully activate the crosslinkers for the 2000-μm-tall microstructures. Postexposure bake was conducted at 95 °C for an hour, with a gentle temperature ramp-up and cool-down to room temperature. A developing process was followed. The sample was carefully placed into the developing solution (propylene glycol monomethyl ether acetate, MicroChem Corp.), where the photoresist side was face down to enhance developing quality and reduce developing time. No agitation was performed during the developing process. The sample was rinsed with isopropyl alcohol (IPA) and dried to complete the pillar fabrication. Figure 6b shows 4-mm tall SU-8 pillar array with the same fabrication process mentioned previously.

Results and applications

Fabrication results of microtowers are presented, including a state-of-the-art 7-mm microtower, diamond-shape 1500-μm-long pillar array, and 2-mm microtower based on a 100-turn toroidal inductor. The 7-mm-tall microtower was fabricated with the following steps. A square photomask pattern with 900-μm sides was prepared for backside exposure. A 7-mm-tall, 3-D-printed bracket was

Kim *et al. Micro and Nano Syst Lett* (2018) 6:14

Page 5 of 9
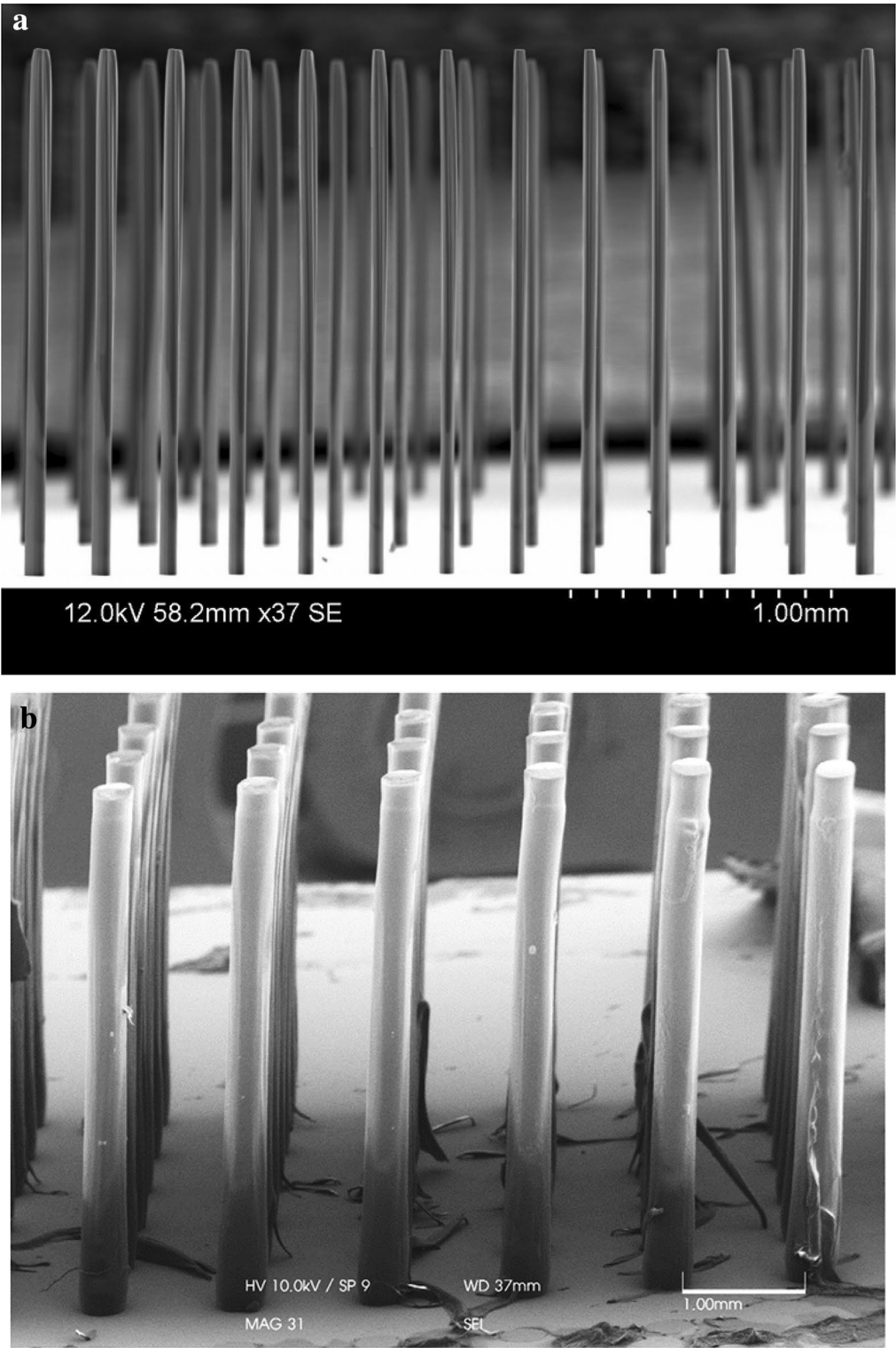
Fig. 6 Array structures of 2000-μm-tall and 4000-μm-tall microtowers; an acrylic filter applied during the UV exposure. Smooth, straight side wall was fabricated

placed on top of the photomask. An SU-8 was poured and baked for approximately 18 h. The sample was exposed to the UV light with the acrylic filter for 850 J/cm^2 where the h-line intensity was around 50 mW/cm^2 with the 283 min exposure time. An additional fan was provided during exposure to keep the sample cooled down as a long time exposure might cause an accumulated heat causing a crosslinking of SU-8. Post-exposure baking was conducted at 95 °C for an hour with gentle temperature raise-up and -down. The sample was developed for an hour in the SU-8 developing solution and rinsed with IPA to complete the fabrication. The 7-mm-tall microtower was successfully fabricated as shown in Fig. 7. To illustrate the versatility of the fabrication, the multidirectional UV lithography scheme [11] was adopted for the fabrication of a diamond-shape, 1500-μm-long tower array as shown in Fig. 8. An array of a 100-μm-hole photo pattern was used for the fabrication. During the UV exposure, three inclined incident exposure angles of $+45°$, $0°$, and $-45°$, respectively, were made by tilting the sample. An SEM image of the fabricated diamond shape in Fig. 8 formed with the structural SU-8 half flare angle of 25° which was as predicted by the Snell's law [11] with an assumption for the refractive index of the SU-8 as 1.67 at an air medium. The maximum half flare angle of the

definable SU-8 is slightly less than 35°, however it could be improved to near 60° by adopting a refractive index matching medium as such glycerol [21]. Despite small artifacts shown in this figure, the fabricated structure has great potential for use as a microfilter in microfluidics.

The proposed microtower fabrication method was applied to a fabrication of 3-D toroidal inductors where the high-aspect-ratio microtower structures will benefit the microdevice performance. Figure 9 shows an optical microscope image of the 100-turn toroid inductors. The fabrication sequence of the 100-turn toroid inductor comprises two major steps: microlithography of SU-8 pillar mold and electroplating for bottom, vertical and top windings. A polar array of 1-mm tall SU-8 pillars were fabricated on a glass substrate as previously described in the fabrication process session [10]. The next step is the fabrication of bottom, vertical and top windings. A seed metal layers of titanium (Ti) and copper (Cu) were deposited on surface of SU-8 pillars as well as the substrate for 30 nm and 500 nm respectively by DC sputter machine. The metal coated sample was spray-coated with NR9-1500PY, a removable negative photoresist from Futurrex, Inc. for 20 μm and baked at 115 °C for 3 min. The sample was UV-exposed to open up the bottom and the vertical winding area
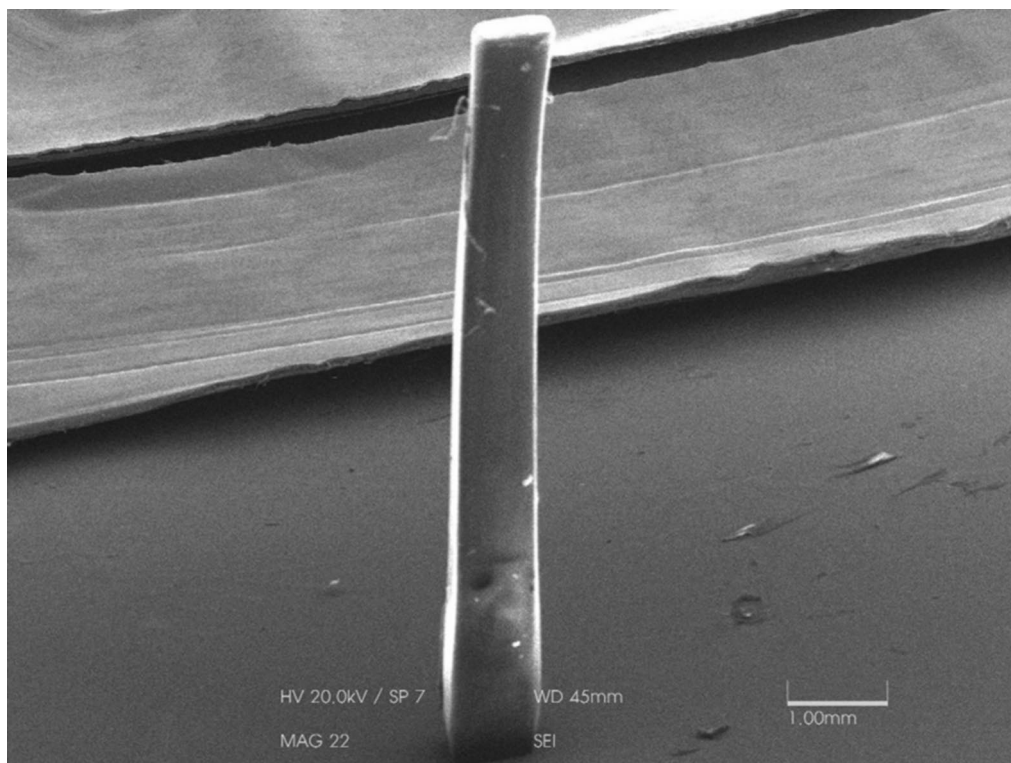

Fig. 7 Seven-millimeter-tall pillar

Kim *et al. Micro and Nano Syst Lett*   (2018) 6:14

Page 7 of 9

at an intensity of 20 mW/cm^2 for 15 s, and followed by a post-exposure bake at 95 °C for minutes. The sample was soaked in RD-6 developer (Futurrex, Inc.) for 90 s and rinsed with deionized (DI) water to be ready for an electroplating. The bottom and vertical winding were simultaneously electroplated for 30 μm in a commercial electrolyte (Copper Mirror Plating Solution, Shor International, Co.) with a current density of 20 mA/cm^2. The NR9-1500PY and the seed metal layers were removed by acetone, hydrochloric solution and hydrofluoric acid respectively to complete the bottom and the vertical windings. Non-photopatternable SU-8 (EPON, Miller-Stephenson, Inc.) was filled up as a thick sacrificial layer to the height of the vertical windings to form a planar surface. After a 500-nm seed Cu layer was deposited by an e-beam evaporator, S1805, a positive photoresist (Shipley LLC.), was spray coated for 15 μm. An electroplating mold for the top winding was patterned by UV exposure and developed (MF-319 developer, Shipley LLC.). Cu was electroplated through the positive photoresist mold for 30 μm. The photoresist mold, Cu seed layer, and the SU-8 filler were etched out by acetone and hydrochloric acid to complete the fabrication of the toroid inductor. Figure 9a shows the bottom, inner vertical, and outer vertical windings with two measurement pads. In Fig. 9b, the inner vertical winding has the smallest microtower diameter of 30 μm

with a 1000-μm height. Figure 9c shows the outer vertical winding of the inductor. A total of 200 microtowers had to fabricate without any failure to complete one inductor. Note that SU-8 microtowers were coated with 30-μm-thick copper for use as electroplating, so the size of the image may look more substantial than 30 μm. Figure 9d shows completed 100-turn toroidal inductors in batch.

Fabricated 100-turn toroidal inductors were electrically characterized as shown in Fig. 10. Characterization data includes inductance, ac resistance, and quality factors over the frequency range of 0.1–100 MHz. Figure 10a shows the inductance and the quality factor over 0.1–100 MHz. An average inductance of 950 nH for the 100-turn inductor was observed. The quality factor in the same graph shows a peak of 22 at 60 MHz. Figure 10b shows the AC resistance measurement over the frequency range of 0.1–100 MHz. Since the 100-turn inductor has longer and narrower conductive lines, the AC resistance appeared relatively high around 5.4 Ω. After 10 MHz, the AC resistances were rapidly increased due to the skin-depth effect and the resonance frequency. As the toroid microinductors has been utilized as a passive component for a small power converters [22–24], the fabricated inductor shows excellent potential for miniaturization of a power inductor in microfeature size
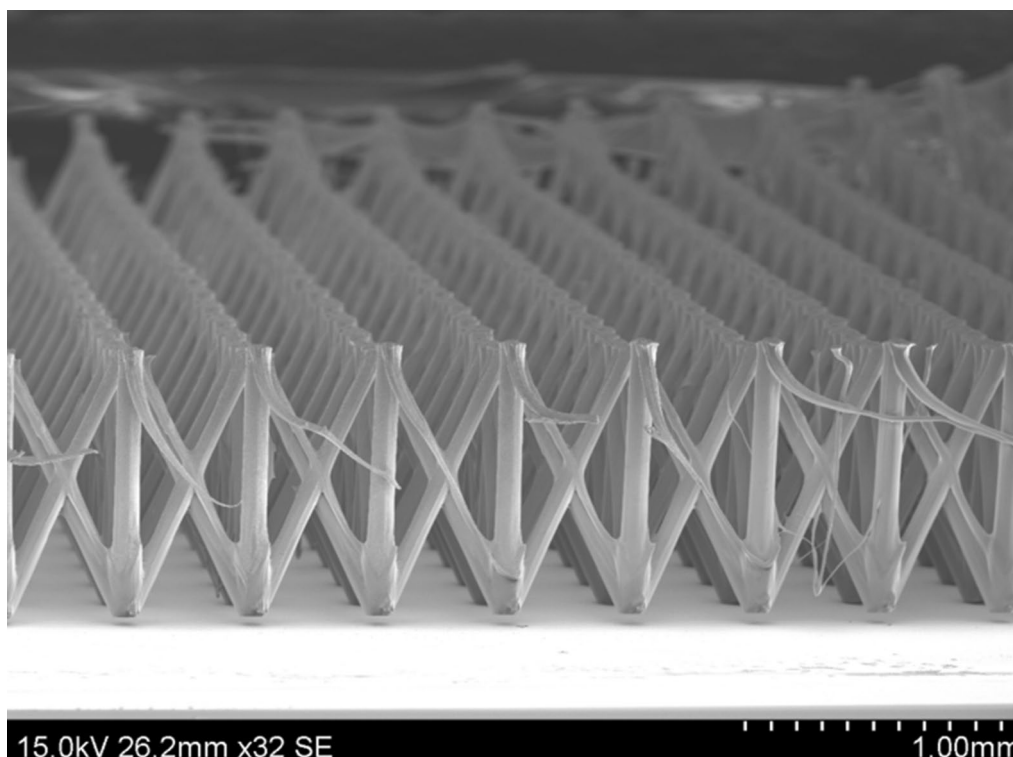
Fig. 8 Diamond-shaped, 1500-μm-long, tower array with potential use of a microfilter device

Kim *et al. Micro and Nano Syst Lett* (2018) 6:14

Page 8 of 9
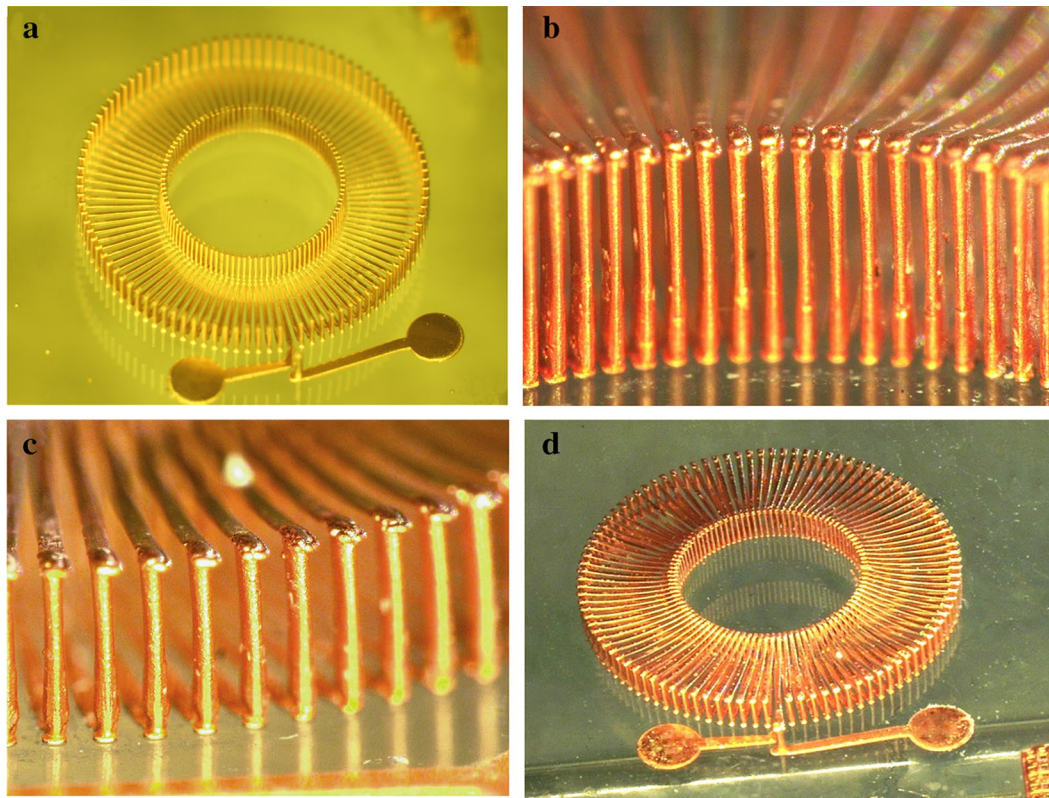
Fig. 9 100-turn toroidal microinductor, **a** bottom and vertical winding, outer diameter is 8 mm; **b** inner vertical winding, height is about 1000 µm; **c** outer vertical winding, the height is about 1000 µm; and **d** a batch fabrication of 100-turn toroidal inductors

without sacrificing its performance and, thereby, reducing the volume of the small power converter.

Conclusion

A fabrication scheme of a high-aspect-ratio, tall microstructure in the height range of 1000 to 7000 µm was introduced. A microstructure with high-aspect-ratio and taller than 1000 µm is named as a microtower, since fabrication of the structure requires a narrow-band single-peak wavelength during the exposure. A spectrum of the UV exposure with an acrylic filter was verified to eliminate the i-line and showed approximately 60% transparency to the h-lines. Since the SU-8 was designed to be crosslinked under UV range, the wavelength region at the h-line was assumed to be reactant to the SU-8. To prove the concept, an array of 2000-µm-tall microtowers were successfully fabricated with a smooth straight sidewall, while a 1000-µm-tall microtower array showed wavy sidewalls without using the acrylic filter during UV exposure. As an alternative 3-D UV exposure scheme, a 1500-µm-long inclined microtower was successfully demonstrated, validating the batch fabrication as well as the process
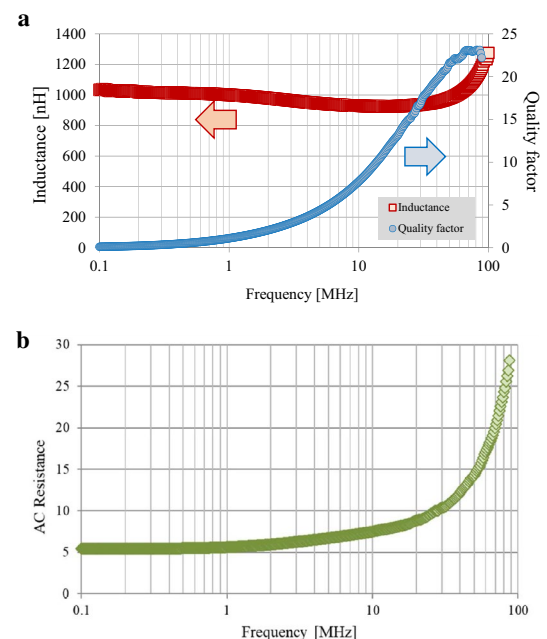
Fig. 10 Characterization results of the 100-turn toroid inductor: inductance, low-frequency resistance, and quality factor

Kim *et al. Micro and Nano Syst Lett*   (2018) 6:14

Page 9 of 9

compatibility with multidirectional UV lithography. A 100-turn toroidal microinductor was fabricated and electrically characterized. Vertical windings were fabricated based on the proposed fabrication scheme with 1000-μm height. An average inductance of 950 nH in the frequency range of 0.1–10 MHz was observed, with a low-frequency resistance of 5.4 Ω and a peak quality factor of 22 at 60 MHz.

Authors' contributions
JK carried out most experiments and drafted the manuscript. HAT and MA conducted and analyzed the light transparency and intensity attenuation data. All the authors discussed the proposed method and experimental results. All authors read and approved the final manuscript.

Publisher's Note
Springer Nature remains neutral with regard to jurisdictional claims in published maps and institutional affiliations.

References
1. Abgrall P, Conedera V, Camon H, Gue AM, Nguyen NT (2007) SU-8 as a structural material for labs-on-chips and microelectromechanical systems. Electrophoresis 28:4539–4551
2. Aekbote BL, Fekete T, Jacak J, Vizsnyiczai G, Ormos P, Kelemen L (2016) Surface-modified complex SU-8 microstructures for indirect optical manipulation of single cells. Biomed Opt Exp 7:45–56
3. Xie X, Livermore C (2016) A pivot-hinged, multilayer SU-8 micro motion amplifier assembled by a self-aligned approach. In: 2016 IEEE 29th international conference on micro electro mechanical systems (MEMS), Shanghai, China, 24–28 Jan. 2016, pp 75–78
4. Dhakar L, Tay FEH, Lee C (2015) Development of a broadband triboelectric energy harvester with SU-8 micropillars. J Microelectromech Syst 24(1):91–99
5. Ghalichechian N, Sertel K (2015) Permittivity and loss characterization of SU-8 films for mm W and terahertz applications. IEEE Antennas Wirel Propag Lett 14:723–726
6. Lorenz H, Despont M, Fahrni N, Brugger J, Vettiger P, Renaud P (1998) High-aspect-ratio, ultrathick, negative-tone near-UV photoresist and its applications for MEMS. Sens Actuators A Phys. 64:33–39
7. Campo AD, Greiner C (2007) SU-8: a photoresist for high-aspect-ratio and 3D submicron lithography. J Micromech Microeng 17:81–95
8. Yoon YK, Pan B, Papapolymerou J, Tentzeris M, Allen MG (2005) Surface-Micromachined Millimeter-wave Antennas. In: The 13th international conference on solid-state sensors, actuators and microsystems, Seoul, Korea, June 5–9 2005, pp 1986–1989
9. Mahanfar A, Lee S, Parameswaran A, Vaughan R (2010) Self-assembled monopole antennas with arbitrary shapes and tilt angles for system-on-chip and system-in-package applications. IEEE Trans Antennas Propag 58(9):3020–3028
10. Kim J, Herrault F, Yu X, Allen MG (2012) Microfabrication of air-core toroidal inductor with very high aspect ratio metal-encapsulated polymer vias. PowerMEMS 2012:30–33
11. Kim J, Allen MG, Yoon YK (2011) Computer-controlled dynamic mode multidirectional UV lithography for 3-D microfabrication. J Micromech Microeng 21(3):1–14
12. Wang M, Ngo K D T, Xie H (2008) SU-8 enhanced high power density MEMS inductors. In: 34th annual conference of IEEE industrial electronics, Orlando, FL, 2008, pp 2672–2676
13. Le HT, Mizushima I, Nour Y, Tang PT, Knott A, Ouyang Z, Jensen F, Han A (2018) Fabrication of 3D air-core MEMS inductors for very-high-frequency power conversions. Microsyst Nanoeng 4(17082):1–9
14. Du LQ, Wang ZZ, Ruan XP, Chen SL, Shan Q (2015) Fabrication of SU-8 microneedle based on backside exposure technology. Key Eng Mater 645–646:853–858
15. Lee JB, Choi KH, Yoo K (2015) Innovative SU-8 lithography techniques and their applications. Micromachines 6:1–18
16. Kang M, Byun JH, Na S, Jeon NL (2017) Fabrication of functional 3D multi-level microstructures on transparent substrates by one step back-side UV photolithography. RSC Adv. 7:13353–13361
17. Yang R, Wang W (2005) A numerical and experimental study on gap compensation and wavelength selection in UV-lithography of ultra-high aspect ratio SU-8 microstructures. Sensors Actuators B 110:279–288
18. Kim J (2018) Fabrication of SU-8 Microtowers for a 100-turn Toroid Inductor. In :IEEE-NEMS 2018, Singapore, April 22–26 2018
19. Kim J, Kim C, Allen MG, Yoon YK (2015) Modeling and fabrication of dynamic mode multidirectional UV lithography for three-dimensional nanostructures. J Micromech Microeng 25(2):1–10
20. Kim J, Yoon YK, Allen MG (2016) Computer numerical control (CNC) lithography: light-motion synchronized UV-LED lithography for 3-D microfabrication. J Micromech Microeng 26(3):1–10
21. Kim J, Yun TS, Jee H, Yoon YK (2009) Adjustable refractive index method for complex microstructures by automated dynamic mode multidirectional UV lithography. In: IEEE 21st international conference on micro electro mechanical systems, 2009. MEMS 2009. Sorrento, Italy, Jan. 2009, pp 733–736
22. Kim J, Kim M, Kim J, Allen MG (2015) Solenoid microinductors with anisotropic nanolaminated CoNiFe cores for high-frequency DC–DC power conversion. In: IEEE international magnetics conference, Beijing, China, May 11–15 2015
23. Allen MG, Araghchini M, Chen J, Alamo JD, Doan-Nguyen V, DesGroseilliers G, Harburg D, Herrault F, Jin D, Kim J, Kim M, Lang J, Levey CG, Lim S, Bin Lu, Murray C, Otten D, Palacios T, Perreault D, Piedra D, Qiu J, Ranson J, Sullivan C, Sun M, Yu X, Yun H (2013) A technology overview of the ARPA-E PowerChip, development program. IEEE Trans Power Electron 28(9):4182–4201
24. Le HT, Nour Y, Han A, Jensen F, Ouyang Z, Knott A (2018) Microfabricated air-core toroidal inductor in very high-frequency power converters. IEEE J Emerg Select Topics Power Electron 6(2):604–613